

Journal of Biomedical Optics

SPIDigitalLibrary.org/jbo

Viscosity measurement based on shear-wave laser speckle contrast analysis

Yi Cheng
Sinan Li
Robert J. Eckersley
Daniel S. Elson
Meng-Xing Tang

Viscosity measurement based on shear-wave laser speckle contrast analysis

Yi Cheng,^a Sinan Li,^a Robert J. Eckersley,^b Daniel S. Elson,^c and Meng-Xing Tang^{a,*}

^aImperial College London, Department of Bioengineering, London, SW7 2AZ, United Kingdom

^bKing's College London, Department of Biomedical Engineering, London, SE1 7EH, United Kingdom

^cImperial College London, Hamlyn Centre for Robotic Surgery, Department of Surgery and Cancer, London, SW7 2AZ, United Kingdom

Abstract. Tissue viscosity is correlated with tissue pathological changes and provides information for tissue characterization. In this study, we report an optical method to track continuous shear-wave propagation at centimeter depths in an optically turbid medium. Shear-wave attenuation coefficients were measured at multiple frequencies using shear-wave laser speckle contrast analysis (SW-LASCA) to quantitatively estimate tissue viscosity using the Voigt model. Shear waves were generated within tissue-mimicking phantoms by an amplitude-modulated ultrasound (modulation frequency: 100 to 600 Hz) and tracked by time-resolved laser speckle contrast difference received on a charged-coupled device camera. Averaged contrast difference over a selected time window was related to shear-wave amplitude and used to calculate the shear-wave attenuation coefficient. Phantoms of varying viscosities (0.1 and 0.3 Pa s) were studied. Attenuation coefficients for different shear-wave frequencies (100 to 600 Hz) were calculated. Derived viscosity values had a maximum standard deviation of 9%, and these values were consistent with the independent measurements reported in a previous study using non-optical methods. © 2013 Society of Photo-Optical Instrumentation Engineers (SPIE) [DOI: 10.1117/1.JBO.18.12.121511]

Keywords: shear wave; laser speckle contrast; viscosity; elasticity; acoustic radiation force; ultrasound.

Paper 130512SSRR received Jul. 20, 2013; revised manuscript received Nov. 19, 2013; accepted for publication Nov. 27, 2013; published online Dec. 19, 2013.

1 Introduction

The mechanical properties of tissue, such as stiffness and viscosity, are often correlated to pathological changes. For example, during the growth of malignant tumors, healthy tissues are often replaced by stiffer fibrotic tissues.¹ In fatty liver disease, large vacuoles of fat accumulate in liver cells, leading to an increase of liver viscosity.² For decades, researchers have been developing tissue viscoelasticity imaging to measure tissue mechanical properties noninvasively and quantitatively. One approach is to push tissue with either a static or dynamic force and to inversely estimate elastic modulus from the resulting tissue response.³ An alternative method is to generate and track shear-wave propagation in tissue and to calculate the elastic modulus by measuring the shear-wave velocity.⁴ This second method suffers fewer boundary effects,⁵ and in addition to the elasticity, tissue viscosity can be evaluated by measuring the shear-wave dispersion, e.g., measuring shear-wave attenuation or velocity at various shear-wave frequencies, and the viscoelasticity can be obtained from the Voigt's model.⁶

Magnetic resonance imaging and ultrasound have shown a good capacity for shear-wave tracking in tissue.^{7,8} However, tracking shear waves with optical methods may bring additional advantages—it is sensitive at the optical wavelength scale and offers the opportunity to combine optical imaging with viscoelasticity imaging, providing complementary optical information for clinical diagnosis. In our previous study,⁹ we proposed an optical method to track transient shear waves at centimeter depth within tissue-mimicking phantoms by shear-wave laser speckle contrast analysis (SW-LASCA). Based on a time-of-flight method, local shear-wave speed was calculated by finding

the time shift of a time-resolved contrast difference signal due to the transient shear waves generated at two locations separated by a certain distance. Elastography of a heterogeneous phantom was then achieved based on the measured shear-wave speeds. In this article, with the same setup, we proposed a method to track continuous shear-wave propagation and to quantify the viscosity of tissue-mimicking phantoms by measuring the dispersion of the shear-wave attenuation. First, the principle of SW-LASCA is briefly introduced, including the methodology and experimental setup. Then, the method to measure shear-wave attenuation dispersion is described, and experiments are conducted on phantoms with various viscosities. The viscosity is then calculated from the measured shear-wave dispersion and compared with the values in literature. Finally, both advantages and limitations for this method are discussed and summarized.

2 Method

The method of SW-LASCA was described in Ref. 9, and a brief summary is provided here. Speckle pattern images are formed when coherent light is transmitted through a turbid medium and detected by a charged-coupled device (CCD) camera. Contrast of speckle pattern images is calculated by

$$C = \frac{\sigma}{\bar{I}}, \quad (1)$$

where σ and \bar{I} are the standard deviation and mean of CCD pixel intensities, respectively. C is close to unity if there is no movement within the medium, and decreases otherwise. In SW-LASCA, shear waves introduce movement of the optical scatterers in an optical turbid medium, and the time-resolved speckle

*Address all correspondence to: Meng-Xing Tang, E-mail: mengxing.tang@imperial.ac.uk

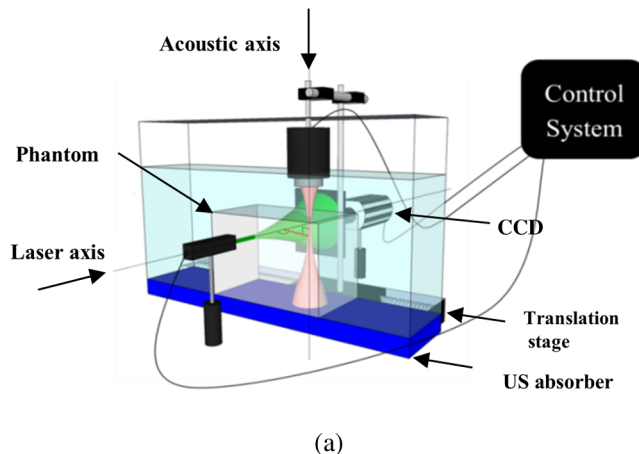
contrast difference (ΔC) is calculated to reveal the shear-wave propagation. The contrast difference (ΔC) is the reduction of the speckle contrast with (C_{SW}) and without (C_{BG}) shear waves:

$$\Delta C = C_{BG} - C_{SW}. \quad (2)$$

Figure 1(a) shows our SW-LASCA setup. The tissue-mimicking phantom was fixed in a perspex tank filled with degassed water. A 532-nm Nd:YAG long-coherence laser (Excelsior 532, Newport Inc., Irvine, CA) illuminated the phantom, and the transmitted laser speckle patterns were recorded on a CCD camera (Qimaging Retiga EXi, Surrey, BC, Canada). The CCD camera was aligned with the laser axis to allow maximized light intensity to be received. Continuous shear waves were generated by an amplitude-modulated ultrasound using a focused ultrasound transducer (Panametric NDT Videoscan 307, 5-MHz central frequency, 5-cm focal length, Olympus, Essex, UK) tens of millimeters away from the optical axis. The full-width-at-half-maximum of the ultrasound focus was 1 cm in the axial direction and 0.1 cm in the lateral direction. Shear waves propagating toward the scattered light region [the green region in Fig. 1(a)] modulate the light and thus the CCD speckle contrast difference signal. Figure 1(b) is a typical time-resolved contrast difference signal due to the continuous shear-wave propagation, where 400-Hz shear waves are generated. The signal was produced by recording CCD speckle images with different time delays (x -axis) after the ultrasound has been launched. As shown, the contrast difference signal varies with the shear-wave frequency over time. The distance between laser and ultrasound axes can be modified by moving the transducer with a translation stage, as shown in Fig. 1(a). Therefore, local shear-wave information, such as speed and attenuation coefficient, could be obtained from the time-resolved contrast difference signals produced by the shear waves originating from two ultrasound locations.⁹

In a viscoelastic medium, such as tissue, shear-wave attenuation may change at different frequencies. This phenomenon is called shear-wave attenuation dispersion. The Voigt model¹⁰ may be used to describe the shear attenuation dispersion as below

$$a(\omega) = \sqrt{\frac{\rho\omega^2(\sqrt{\mu_1^2 + \omega^2\mu_2^2} - \mu_1)}{2(\mu_1^2 + \omega^2\mu_2^2)}}, \quad (3)$$



where $a(\omega)$ (m^{-1}) is the shear-wave attenuation coefficient, ω (rad/s) is the angular frequency of the shear wave, and ρ (kg/m^3), μ_1 (Pa), μ_2 (Pa s) are tissue density, elasticity, and viscosity, respectively. If $a(\omega)$ is measured at different shear-wave frequencies, elasticity and viscosity can be estimated with Eq. (3).

To measure the shear-wave attenuation with the time-resolved speckle contrast difference signals, the following relationships are deduced. First, the relationship between shear-wave attenuation coefficient and amplitude is obtained as

$$A_i = A_0 \exp(-\alpha_f S_i), \quad (4)$$

where A_i is the shear-wave amplitude at position i , A_0 is the initial amplitude of shear wave at the ultrasound focus, α_f is the attenuation coefficient of the shear wave at frequency f , and S_i is the shear-wave path length between the focus and the position i . According to Eq. (4), the shear-wave attenuation coefficient could be derived if A_i , A_0 , and S_i are known.

In the experiments, S_i , which is the distance between the laser and ultrasound axes, is known. A_0 is assumed to be linear with the magnitude of the acoustic radiation force (ARF), and the ARF is proportional to the time-averaged ultrasound intensity I_0 .¹¹ Therefore, the relationship between shear-wave initial amplitude A_0 and I_0 can be related as

$$I_0 = K A_0, \quad (5)$$

where K is a constant. On the other hand, the time-averaged ultrasound intensity, I_0 , is proportional to the mean square of the ultrasound pressure. With a hydrophone measurement, I_0 could be further related to the input voltage of ultrasound transducer. Figure 2 shows the hydrophone measurement result (red dots), where the x -axis is the ultrasound input voltage and the y -axis is the ultrasound intensity (mean square of acoustic pressure). With linear regression (blue solid curve), the relationship between the time-averaged ultrasound intensity and the transducer input voltage (between 300 and 600 mVpp) was found to be

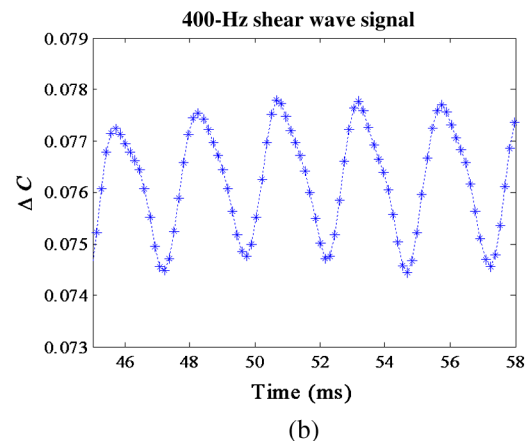


Fig. 1 (a) Shear-wave laser speckle contrast analysis (SW-LASCA) experimental setup. (b) Time-resolved speckle contrast difference to track shear wave.

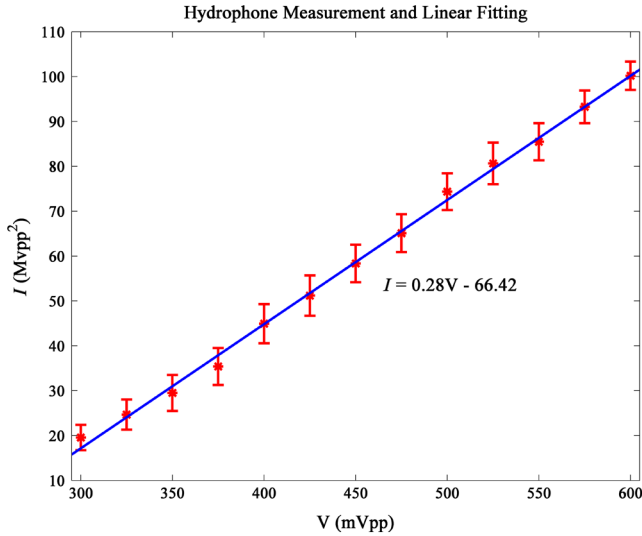


Fig. 2 Hydrophone measurement result.

$$I_0 = 0.28V - 66.42. \quad (6)$$

By substituting Eqs. (5) and (6) into Eq. (4), we can obtain

$$A_i = \frac{0.28V - 66.42}{K} \exp(-\alpha_f S_i). \quad (7)$$

In Eq. (7), A_i and K are unknown, and α_f is the averaged attenuation coefficient over S_i . In order to eliminate K and to calculate the local shear-wave attenuation coefficient, shear waves were generated at two locations with path lengths of S_i and S_j . The ratio of the corresponding shear-wave amplitudes is calculated as

$$\frac{A_i}{A_j} = \frac{0.28V_i - 66.42}{0.28V_j - 66.42} \exp[-\alpha_f (S_i - S_j)]. \quad (8)$$

In Eq. (8), the unknown constant K is eliminated. To calculate the left side of Eq. (8), we assume that the identical shear-wave amplitudes at the detection position result in identical contrast differences, which means if $\Delta C_i = \Delta C_j$, then $A_i = A_j$, despite of the original position of the shear waves. Consequently, Eq. (8) can be rewritten as

$$\left\{ 1 = \frac{0.28V_i - 66.42}{0.28V_j - 66.42} \exp[-\alpha_f (S_i - S_j)] \right\}_{\Delta C_i = \Delta C_j}, \quad (9)$$

and the shear-wave attenuation coefficient α_f at frequency f can be calculated by

$$\left\{ \alpha_f = \frac{\log \frac{0.28V_i - 66.42}{0.28V_j - 66.42}}{S_i - S_j} \right\}_{\Delta C_i = \Delta C_j}. \quad (10)$$

Below, we describe how we found (V_i, V_j) pair in Eq. (10). Figure 3 shows the relationship between ultrasound input voltage $V_{i(j)}$ and contrast difference $\Delta C_{i(j)}$ induced by a 400-Hz shear wave, in which the markers are the mean values of the contrast difference signals over time [e.g., averaged value from Fig. 1(b)]. P1 and P2 are the two positions where shear waves are generated. Because P2 is located further away

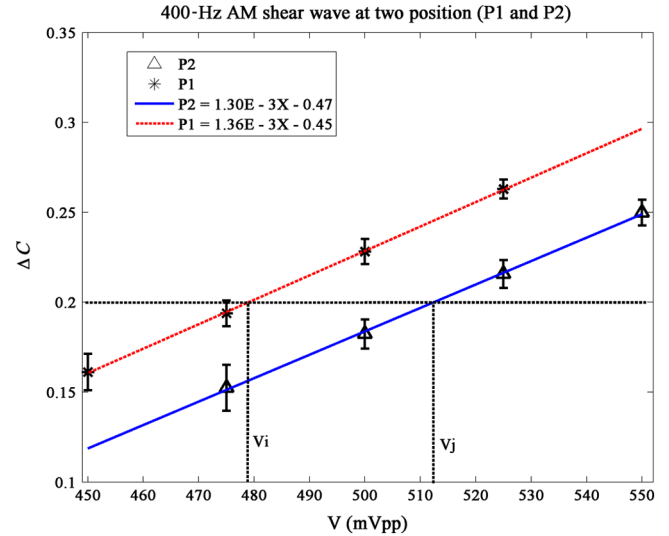


Fig. 3 Relationship between input voltage of ultrasound transducer and mean speckle contrast difference. Shear-wave frequency is 400 Hz.

from the detection area than P1, the corresponding mean contrast difference values are generally smaller because of the shear-wave attenuation. By changing the ultrasound input voltage, the mean contrast differences increase for both P1 and P2. Solid lines in the figure indicate linear regressions of the data. As indicated by the dashed lines in the figure, for a given ΔC , V_i and V_j can be obtained from the fitted curves to calculate the shear-wave attenuation coefficient α_f using Eq. (10).

Shear waves can be generated by the ARF resulting from the momentum transfer from the ultrasound field.¹² In the experiment, continuous shear waves were generated by an oscillatory ARF via modulating the amplitude of ultrasound over time. Shear-wave frequencies were determined by the amplitude modulation frequency ranging from 100 to 600 Hz. Figure 4 is the schematic of the experimental setup. The green area is the photon probability density mapping of scattered light in the phantom predicted by Monte Carlo simulation¹³ using a million photons to get a good statistics of the photon probability density mapping, where a 6-mm radius detection area was defined to match the experiment. The parameters in the Monte Carlo simulation were determined based on Ref. 14

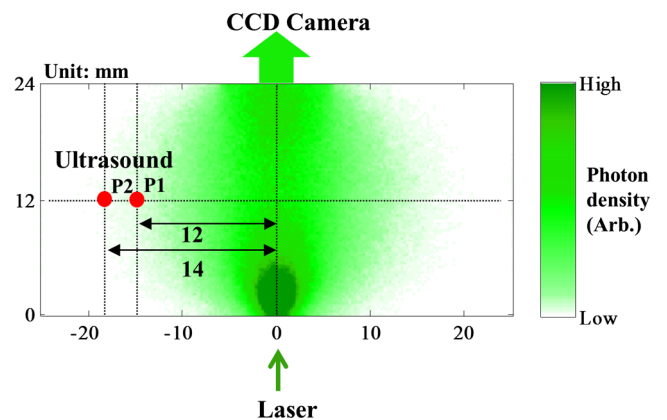


Fig. 4 Schematic for detecting continuous shear waves with SW-LASCA method.

Table 1 Attenuation coefficients over shear-wave frequency.

Frequency	100 Hz	200 Hz	300 Hz	400 Hz	500 Hz	600 Hz
#1 (m^{-1})	44.56 ± 2.18	70.63 ± 5.10	90.36 ± 1.93	116.18 ± 7.80	121.62 ± 3.01	126.74 ± 2.50
#2 (m^{-1})	7.53 ± 1.76	17.54 ± 3.92	30.20 ± 4.58	36.43 ± 2.74	41.42 ± 4.74	47.50 ± 4.17

including optical absorption coefficient $\mu_a = 0.2 \text{ cm}^{-1}$, optical scattering coefficient $\mu_s = 30 \text{ cm}^{-1}$, and anisotropic coefficient $g = 0.8$. Shear waves were generated at P1 and P2 with amplitude-modulated ultrasound and tracked by the time-resolved contrast difference signal [e.g., Fig. 1(b)]. The attenuation coefficients of shear wave at each frequency were then calculated with Eq. (10).

The tissue-mimicking phantoms used in the experiment were made of 4% gelatin and 1% agar following the recipe in Ref. 15. A 4% intralipid was added in the solution to obtain a reduced optical scattering coefficient of 5 cm^{-1} .¹⁴ In order to alter viscosity of the phantom, 0.3% Xanthan gum was added in one of the phantom (#1). The size of phantoms was $120 \times 35 \times 24 \text{ mm}^3$, and both phantoms were made to be homogeneous.

3 Result

Table 1 shows the shear-wave attenuation coefficients measured in the experiment. Standard deviations were produced from three repeated measurements. As expected, the shear-wave attenuation dispersion is observed on both phantoms. Shear-wave attenuation increases with the increase of shear-wave frequency. The phantom with higher viscosity (#1) has a larger attenuation coefficients compared with the less viscous phantom (#2). Furthermore, according to Table 1, the standard deviation of attenuation coefficient measured with our method ranges from 2% to 23%.

Equation (3) was used to calculate viscosity of phantoms with the shear-wave attenuation coefficients in Table 1 and a constrained elasticity range (within 6 kPa) estimated with the method in our previous article.⁹ Table 2 shows that the viscosities measured in the experiment (Row 2) agree with the reference values in Ref. 15 (Row 3) and have a maximum standard deviation of 9%.

4 Discussion and Conclusion

This study shows promising results of viscosity measurements in tissue-mimicking phantoms by SW-LASCA. The prior information on elasticity can be obtained by measuring the shear-wave speed described in Ref. 9. These two methods are based on the same setup; therefore, it is easy to switch between them.

Because of the small wavelength of light, the sensitivity of shear-wave tracking with SW-LASCA could be better than ultrasound-based methods. In addition, optical detection inherently enables the detected signal to contain optical property

Table 2 Comparison of our result with reference value.

Phantom	#1	#2
Experiment result (Pa s)	0.12 ± 0.01	0.35 ± 0.02
Reference value (Pa s)	0.10 ± 0.02	0.30 ± 0.05

information. In the future, we will combine the SW-LASCA and ultrasound-modulated optical tomography¹⁶ to build a dual-mode imaging system sensitive to both mechanical and optical contrasts. With the complementary information provided by optical detection, it could potentially be used as a diagnosis tool for cancerous tissues.

The previously reported ultrasound-based method had a bias of $\sim 6\%$ on viscosity measurement.^{10,15} Our method shows a bias of $\sim 17\%$. One possible reason is the variation of phantoms even though we followed the recipe used in previous reports. Furthermore, there are two additional factors. First, shear-wave reflection at phantom boundaries may affect the measured contrast difference values and, thus, the results in the bias on the attenuation coefficient estimation. In the experiment, the phantom was fixed within a water tank made of Perspex. Due to large shear impedance mismatch between the Perspex and the phantom, shear waves were almost totally reflected at the Perspex-phantom interface. Therefore, both the original and reflected shear waves contributed to the contrast difference signal, and this may bias the estimation of the shear-wave attenuation coefficient. However, this artificially strong shear-wave reflection in the experiments may not occur in real applications. Second, in Eq. (9), we assumed that the identical shear-wave amplitudes at detection point result in identical contrast differences, even if the shear waves originate from two positions along the propagation path. This assumption may not be totally true due to shear-wave diffraction: the shear wave with a longer propagation distance will overlap more with the scattered light and so generates a different contrast difference amplitude compared with the shear wave propagated a shorter distance. This effect could be minimized either by generating plane shear waves, so that

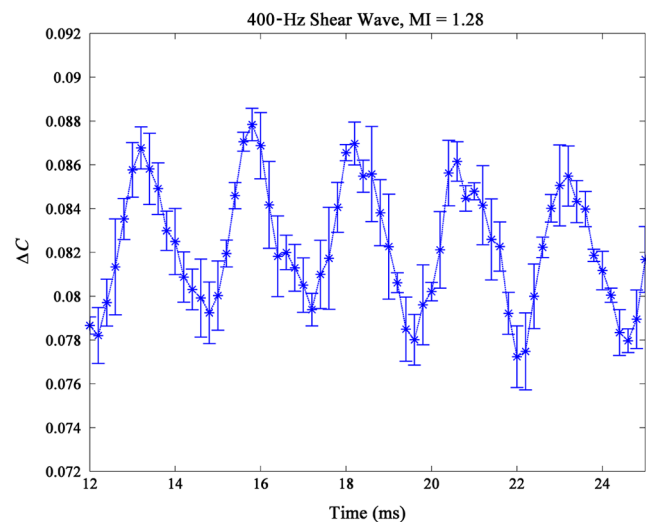


Fig. 5 Speckle contrast difference due to continuous shear wave generated by an ultrasound mechanical index (MI) of 1.28. Standard deviation is produced with three repeated measurements.

less shear wave-spreading will be encountered, or by decreasing the distance between the two locations, so that the change of shear-wave geometry may be ignored.

In this feasibility study, relatively high intensities of ultrasound were used in the experiments to generate shear waves. A mechanical index (MI) of 1.9 is usually recognized as the upper limit for clinical ultrasound use. Therefore, a MI of 1.28 was applied to prove the feasibility of reducing ultrasound intensity for the measurement. The same setup and system parameters were used to obtain Fig. 5, except for a lower ultrasound intensity. In Fig. 5, we used an ultrasound pressure equivalent to a MI of 1.28 at 5 MHz to generate shear waves, which is well below the ultrasound safety limit. Results show a good signal-to-noise ratio at $MI = 1.28$. The standard deviation is produced from the three repeated measurements.

In laser speckle contrast measurements, the CCD exposure time is important. On one hand, we hope to use a short enough CCD exposure time to minimize the speckle decorrelation effect due to blood flow and other tissue motions. On the other hand, we want to use a long enough CCD exposure time to maximize the light intensity received on the CCD in order to get a better signal-to-noise ratio. Generally, an exposure time less than 0.5 ms leads to a noisy signal, and an exposure time larger than 10 ms leads to 50% reduction of contrast in our measurements. Therefore, 2-ms exposure time is usually used in the experiments. However, this exposure time could be further reduced for *in vivo* measurements, where speckle decorrelation time is much shorter than 10 ms. In the future, it would also be interesting to evaluate to what extent the shear-wave signal will be affected by the speckle decorrelation by using a flow phantom.

Phantoms in the study simulated the scattering properties of tissue with a thickness of 24 mm and a reduced optical scattering coefficient of about 5 cm^{-1} for the 532-nm laser.¹⁷ The reduced optical scattering coefficient was relatively weak compared with that of some biological tissues like breast.¹⁸ Therefore, further investigations are needed to assess the feasibility of our method on biological tissues. In addition, the green laser used in the current study will be replaced by a near-infrared laser for a better penetration depth in biological tissues.

Currently, we used one single element transducer to generate shear waves at two positions by translating the transducer to different positions. In the future, we will program a linear array transducer to replace the “mechanical” translation to “electrical” translation by dynamic ultrasound beam focusing. Dynamic beam focusing will provide a faster and more flexible measurement.

In summary, we proposed an optical method to quantitatively measure the viscosity at centimeter depth within tissue-mimicking phantoms. It is potentially more sensitive to viscosity changes than ultrasound-based methods, because the light wavelength is much smaller than that of the ultrasound. It may also complement viscoelastography techniques based on ultrasound or magnetic resonance imaging by providing optical information of tissues. By combining SW-LASCA with ultrasound-modulated optical tomography, we aim to build a dual-mode imaging system that is sensitive to both mechanical and optical contrasts. However, further investigation is needed to assess the feasibility of this method *in vivo*, where the speckle decorrelation time is short and the optical scattering coefficient is large.

Acknowledgments

The authors want to thank Professor David O. Cosgrove for fruitful discussion, and EPSRC (EP/H02316X/1), the Royal

Society, and China scholarship council for financial support. The correspondence should be made to M.X.T and D.S.E (mengxing.tang/daniel.elson@imperial.ac.uk).

References

1. D. Cosgrove et al., “Shear wave elastography for breast masses is highly reproducible.” *Eur. Radiol.* **22**(5), 1023–1032 (2012).
2. N. Salameh et al., “Early detection of steatohepatitis in fatty rat liver by using MR elastography,” *Radiology* **253**(1), 90–97 (2009).
3. J. Bamber et al., “EFSUMB guidelines and recommendations on the clinical use of ultrasound elastography. Part 1: basic principles and technology,” *Ultraschall Med.* **34**(02), 169–184 (2013).
4. K. Nightingale, S. McAleavey, and G. Trahey, “Shear-wave generation using acoustic radiation force: in vivo and ex vivo results,” *Ultrasound Med. Biol.* **29**(12), 1715–1723 (2003).
5. M. L. Palmeri and K. R. Nightingale, “Acoustic radiation force-based elasticity imaging methods,” *Interface Focus* **1**(4), 553–564 (2011).
6. C. Shigao et al., “Shearwave dispersion ultrasound vibrometry (SDUV) for measuring tissue elasticity and viscosity,” *IEEE Trans. Ultrason. Ferroelectr. Freq. Control* **56**(1), 55–62 (2009).
7. A. E. Bohte et al., “MR elastography of the liver: defining thresholds for detecting viscoelastic changes,” *Radiology* **269**(3), 768–776 (2013).
8. J. M. Hudson et al., “Inter- and intra-operator reliability and repeatability of shear wave elastography in the liver: a study in healthy volunteers,” *Ultrasound Med. Biol.* **39**(6), 950–955 (2013).
9. Y. Cheng et al., “Shear wave elasticity imaging based on acoustic radiation force and optical detection,” *Ultrasound Med. Biol.* **38**(9), 1637–1645 (2012).
10. S. Chen, M. Fatemi, and J. F. Greenleaf, “Quantifying elasticity and viscosity from measurement of shear wave speed dispersion,” *J. Acoust. Soc. Am.* **115**(6), 2781–2785 (2004).
11. G. R. Torr, “The acoustic radiation force,” *Am. J. Phys.* **52**(5), 402–408 (1984).
12. V. G. Andreev et al., “Observation of shear waves excited by focused ultrasound in rubber-like medium,” *Acoust. Phys.* **43**(2), 123–128 (1997).
13. L. Wang, S. L. Jacques, and L. Zheng, “MCML—Monte Carlo modeling of light transport in multi-layered tissues,” *Comput. Meth. Prog. Biomed.* **47**(2), 131–146 (1995).
14. H. J. van Staveren et al., “Light scattering in Intralipid-10% in the wavelength range of 400–1100 nm,” *Appl. Opt.* **30**(31), 4507–4514 (1991).
15. J. Bercoff et al., “The role of viscosity in the impulse diffraction field of elastic waves induced by the acoustic radiation force,” *IEEE Trans. Ultrason. Ferroelectr. Freq. Control* **51**(11), 1523–1536 (2004).
16. R. Li et al., “Effects of acoustic radiation force and shear waves for absorption and stiffness sensing in ultrasound modulated optical tomography,” *Opt. Express* **19**(8), 7299–7311 (2011).
17. K. Daoudi, A.-C. Boccara, and E. Bossy, “Detection and discrimination of optical absorption and shear stiffness at depth in tissue-mimicking phantoms by transient optoelastography,” *Appl. Phys. Lett.* **94**(15), 154103 (2009).
18. T. Durduran et al., “Bulk optical properties of healthy female breast tissue,” *Phys. Med. Biol.* **47**(16), 2847–2861 (2002).

Yi Cheng received her BEng degree from Tianjin University, China, with a specialization in opto-electronic engineering in 2010. In 2009 she visited University of Dundee, UK, and worked on the development of an ultrasonic needle for surgery. She is now achieving her PhD degree at Imperial College London, UK, working on optical shear wave elastography for early cancer detection and ultrasound modulated optical tomography for deep tissue imaging. She has developed a dual mode optical system that is sensitive on both tissue mechanical and optical contrast.

Sinan Li joined Imperial College London as a PhD student in biomedical engineering in 2011. He is working on ultrasound mediated optical tomography, optical shear wave elastography, optical sensing of acoustic waves in turbid medium, and phase-transition contrast agents and their applications in ultrasound and optical imaging. He also carries out research on multiply scattering of light and laser speckle statistical analysis. He has developed a Monte Carlo

simulation for laser speckle contrast detection of shear wave in an optically turbid medium.

Daniel Elson is a reader in surgical imaging in the Hamlyn Centre for Robotic Surgery, Institute of Global Health Innovation and Department of Surgery and Cancer at Imperial College London and St. Mary's Hospital. His research interests are based around the development and application of photonics technology to medical imaging, including multispectral endoscopy, ultrasound mediated optical tomography, endoscopic structured lighting, light sources in endoscopy, and polarized endoscopic imaging.

Mengxing Tang joined the Department of Bioengineering, Imperial College as a lecturer in 2006 and became a senior lecturer in 2011. Before moving to London, he was a departmental lecturer in the Department of Engineering Science, University of Oxford. He founded the Ultrasound Imaging Group at Imperial College in 2006 in close collaboration with Dr. Robert Eckersley from KCL. His main research interest is to develop new imaging, image analysis, and sensing techniques with ultrasound, microbubbles and light and apply them to a range of applications, including the diagnosis and treatment of cardiovascular diseases and cancer. He has authored 50 peer-reviewed journal papers.